



# Enhanced Thermal Performance of Parabolic Through Collectors with TiO<sub>2</sub> Nanofluids in An Arid Climate

Mohammed Abdelkrim Belhadi<sup>1</sup>, Mahfoud Kadja<sup>1</sup>, Farid Mechighel<sup>1,2</sup>, Abderrahmane Khechekhouch<sup>3,\*</sup>,

Youcef Hamaiti<sup>4</sup>

<sup>1</sup> University of Constantine 1, Constantine, Algeria

<sup>2</sup> Badji Mokhtar - Annaba University, Annaba, Algeria

<sup>3</sup> University of El Oued, Algeria, El Oued, Algeria

<sup>4</sup> University of Bab-Ezzouar, Algiers, Algeria

\*Correspondence: E-mail: [khechekhouch-abderrahmane@univ-eloued.dz](mailto:khechekhouch-abderrahmane@univ-eloued.dz)

## ABSTRACT

Solar energy is a crucial renewable resource, yet its efficient utilization remains a challenge because conventional heat transfer fluids have limited thermal conductivity. Parabolic Trough Collectors (PTCs) offer a viable solution for solar thermal energy conversion, but optimizing performance is essential for improving efficiency. This study investigates the performance of a PTC using a 0.3% TiO<sub>2</sub>-water nanofluid compared to distilled water (DW) under real environmental conditions in Algeria's arid climate. Two identical PTCs were tested outdoors at flow rates of 0.2, 0.3, and 0.4 L/min to evaluate heat transfer efficiency. The results demonstrated that the nanofluid consistently outperformed DW because of its superior thermal conductivity and heat retention. At 0.4 L/min, the nanofluid achieved 40% thermal efficiency, 9% higher than DW. However, as the flow rate decreased, the efficiency gap narrowed. These findings confirm the potential of nanofluids to enhance solar energy utilization, supporting sustainable energy solutions in high-irradiance regions.

## ARTICLE INFO

### Article History:

Submitted/Received 24 Nov 2024

First Revised 28 Dec 2024

Accepted 05 Feb 2025

First Available Online 06 Feb 2025

Publication Date 01 Apr 2025

### Keyword:

Field experiment in arid climate,  
Heat transfer enhancement,  
Parabolic trough collectors,  
Solar energy efficiency,  
TiO<sub>2</sub> Nanofluids.

## 1. INTRODUCTION

In solar thermal energy systems, heat transfer efficiency largely depends on the design and performance of solar collectors. These devices act as the primary interface between incident solar radiation and the working fluid, facilitating the conversion of radiative energy into thermal energy. Flat plate collectors, known for their simple design and diffuse absorption of radiation, are commonly used in low-temperature applications, where the working fluid is heated through conduction and convection. In contrast, concentrating solar collectors, such as parabolic trough collectors, use reflective surfaces to focus direct normal irradiance onto a receiver, enabling higher temperatures suitable for medium- to high-temperature applications. The thermal efficiency of these collectors is influenced by factors such as optical characteristics, heat loss mechanisms, and the thermodynamic properties of the working fluid. Therefore, optimizing collector design is essential for maximizing overall system performance and ensuring efficient utilization of solar energy. Parabolic solar concentrators represent a promising technology for harnessing solar energy, focusing sunlight onto a linear receiver to generate intense heat. This concentrated energy heats a transfer fluid, enabling its use in a variety of applications such as electricity generation through steam production in solar thermal power plants, industrial process heating, and solar distillation for pure water production. These systems, built with parabolic mirrors that reflect and focus solar radiation, are known for their inherent storage capacity and minimal greenhouse gas emissions [1-3]. Operating efficiently in a temperature range of 60 to 400°C, they offer a versatile solution for medium- and high-temperature applications. Although their annual efficiency is typically between 14 and 22%, their potential for sustainable energy production remains significant [4].

Solar concentrators, which offer a pollution-free alternative, harness this energy through systems such as point collectors (heliostatic and parabolic field) and linear collectors (linear Fresnel and parabolic trough collectors), finding applications in domestic and industrial environments, especially in regions with high direct solar radiation [5]. Among these, the parabolic trough collector (PTC) stands out for its efficient linear concentration of solar radiation onto a heat transfer fluid, which is then used in various applications [6]. While these systems offer a promising avenue, the parabolic solar collector typically achieves an annual efficiency of between 14 and 22% [7], highlighting the continued need for progress to further improve their performance.

Recent studies have explored various methods to enhance PTC performance. Numerical and experimental analyses have demonstrated that optimizing PTC design parameters, such as absorber tube diameter and length, can significantly impact efficiency [8-10]. Additionally, nanofluids (heat transfer fluids containing dispersed nanoparticles) can improve thermal conductivity and heat retention [11].  $\text{Al}_2\text{O}_3$ /water nanofluids at a concentration of 0.2% improved thermal efficiency by 32.1%, compared to pure water at a flow rate of 1 L/min [12].  $\text{Al}_2\text{O}_3/\text{H}_2\text{O}$  and  $\text{Fe}_2\text{O}_3/\text{H}_2\text{O}$  nanofluids at a concentration of 0.30% compared to water and a flow rate of 2 L/min improved efficiency by 13 and 11%, respectively [13]. Further, mixing a carbon nanotube (CNT) coated receiver tube with  $\text{Al}_2\text{O}_3$  nanofluids at a concentration of 0.05% resulted in a 3% increase in overall efficiency [14]. The maximum efficiency reached 57.7% using  $\text{Al}_2\text{O}_3$  nanofluids at a volume concentration of 1%, which strongly depended on the solar incidence angle while the use of a hybrid nanofluid composed of  $\text{Al}_2\text{O}_3$  and CuO reported a 31% improvement in efficiency [15,16]. The use of metal oxide nanofluids (i.e. CuO,  $\text{SiO}_2$ ,  $\text{Al}_2\text{O}_3$ , and  $\text{TiO}_2$ ) at a volumetric concentration of 4% in Therminol VP-1™ improved the thermal performance of parabolic trough solar collectors (PTSCs), validating a thermal model

with low error rates (0.184% experimental, 0.29% theoretical). The nanofluids improved the thermal efficiency compared to pure Therminol VP-1™, with CuO/Therminol VP-1™ demonstrating the highest increase of 1.03%, and also led to increased outlet temperatures: 9.57% for CuO, 6.04% for TiO<sub>2</sub>, 5.21% for Al<sub>2</sub>O<sub>3</sub> and 3.08% for SiO<sub>2</sub> [17]. Water-based (alumina) multi-walled carbon nanotubes (MWCNTs) at various mass concentrations ranging from 0.1 to 0.3 and fixed mass flow rates of 0.012 kg/s and 0.024 kg/s, the maximum thermal efficiencies were 40% for distilled water (DW), 56% for Al<sub>2</sub>O<sub>3</sub>-water, and 58% for CNT-water nanofluids [18]. Work on CuO-H<sub>2</sub>O and SiO<sub>2</sub>-H<sub>2</sub>O nanofluids showed an increase in efficiency between 6.68% and 9% [19,20].

The novelty of this work lies in its real-world application, providing crucial data on the performance of nanofluids in high solar irradiance and extreme temperatures. Unlike previous studies that relied on controlled environments, this research offers practical insights into the feasibility of implementing nanofluids in large-scale solar power installations. The results contribute to the advancement of CSP technology by demonstrating how nanofluids can enhance energy efficiency in arid climates, making solar thermal energy a more viable and sustainable option for regions with abundant solar resources.

## 2. METHODS

### 2.1. Experience Setup

**Figure 1** illustrates a direct comparative study of two locally manufactured parabolic trough solar concentrators, each measuring 1 m in length, with a reflective sheet, as shown in the figure. The two collectors were placed side by side under direct sunlight on a clear day in El Oued City, southeastern Algeria. This configuration facilitated a controlled experiment to isolate the effect of TiO<sub>2</sub> nanoparticles on concentrator performance. One prototype used water enriched with TiO<sub>2</sub> nanoparticles, while the other used pure water, enabling a direct assessment of the nanoparticles' impact under identical environmental conditions.



**Figure 1.** PTCs used in the experiment.

To refine the experiment, two identical PTCs were used, each equipped with a 20 mm internal diameter copper absorber tube to ensure efficient heat transfer. A closed-loop system was implemented, allowing precise control of volumetric flow rates at 0.2, 0.3, and 0.4 L/min. This setup was designed to accurately determine the maximum efficiency of the PTCs under real-world conditions, providing quantitative data to support visual observations regarding the influence of TiO<sub>2</sub> nanoparticles on concentrator performance.

Temperature values were collected using thermocouples positioned at different locations along the two cylinder-parabolic collectors. The combined visual and experimental data provided an in-depth analysis of the effectiveness of nanoparticles in improving solar concentrator efficiency.

## 2.2. Schematic Representation

**Figure 2** provides a schematic representation of the experimental setup designed to analyze the performance of a parabolic trough collector (PTC). The diagram illustrates a closed-loop system, where a pump circulates the working fluid through the device. The fluid was initially drawn from a small reservoir and propelled toward the PTC, a key component for harnessing solar energy. Upon entering the PTC, the fluid was heated as it flowed through the absorber tube, which was positioned along the focal line of the parabolic trough. The heated fluid then exited the PTC and was directed to a larger reservoir.

Temperature sensors, labeled “1” and “2,” were strategically placed at the inlet and outlet of the PTC, respectively, to measure the fluid temperature before and after passing through the collector. These measurements were crucial for determining the heat gain and thermal efficiency of the PTC. A control valve, labeled “3,” was positioned at the outlet of the PTC to regulate the fluid flow rate. This control was essential for maintaining consistent experimental conditions and studying the impact of flow rate variations on PTC performance.

The larger reservoir served as a storage tank, holding the heated fluid before it was recirculated to the pump, completing the closed-loop system. This configuration enabled continuous operation, allowing for long-term experimentation and comprehensive data collection on the thermal behavior of the PTC under different operating conditions.

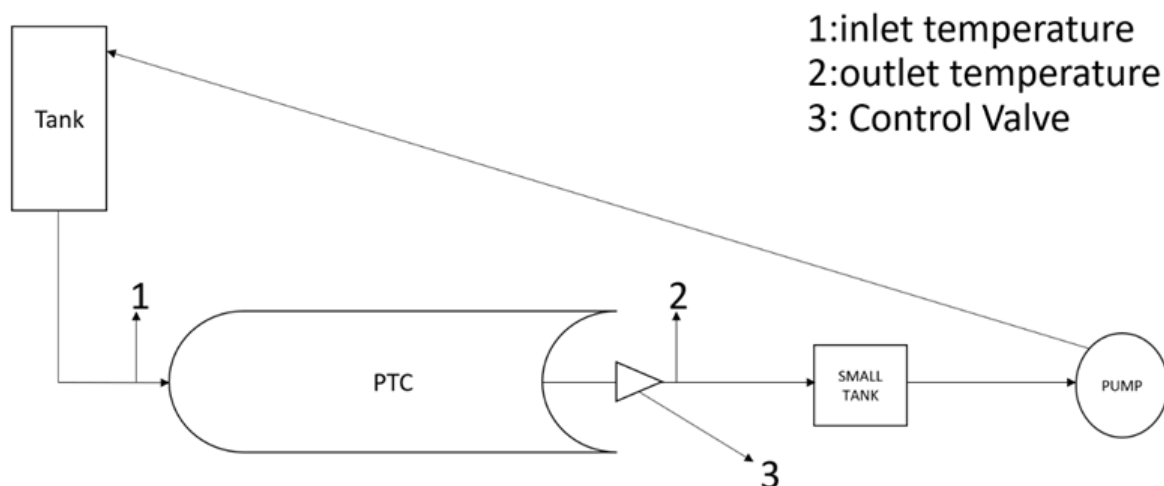


**Figure 2.** Schematic diagram of the experimental setup for solar collectors.

## 2.3. Parabolic Specifications

**Table 1** presents the detailed specifications of the parabolic trough collectors (PTCs) used in this study, providing a comprehensive overview of their physical and operational

parameters. Each PTC measured 0.932 m in length and 0.6 m in width, defining the overall dimensions of the collector and the effective solar radiation capture surface. The edge angle, a critical parameter that determines the acceptance angle of the collector, was set at 125°, indicating the range of incidence angles at which the collector could efficiently concentrate sunlight. The focal length was measured at 0.1 m, dictating the distance at which the concentrated sunlight was focused onto the receiver. The receiver, responsible for absorbing the concentrated solar energy, was constructed of copper with an inner diameter of 20 mm and an outer diameter of 22 mm, ensuring efficient heat transfer to the working fluid. The use of copper as the absorbing material was advantageous because of its high thermal conductivity, which enhanced the collector's ability to convert solar radiation into heat. The table also indicates a concentration ratio of 8.69, reflecting the extent to which the PTC intensified sunlight onto the receiver. This ratio served as a key performance indicator, demonstrating the collector's capability to achieve high operating temperatures, making it suitable for various thermal applications. Overall, **Table 1** provides a concise yet detailed summary of the PTC's design and operational characteristics, offering essential information for evaluating its thermal performance and applicability.

**Table 1.** Specifications of the PTCs used in the experiment.

| Specification                     | Unit    | PTC Value |
|-----------------------------------|---------|-----------|
| Length                            | M       | 0.932     |
| Width                             | M       | 0.6       |
| Rim Angle                         | Degrees | 125       |
| Focal Length                      | M       | 0.1       |
| Receiver Inside Diameter (DiD_i)  | mm      | 20        |
| Receiver Outside Diameter (DoD_o) | mm      | 22        |
| Absorber Metal                    | -       | Copper    |
| Concentration Ratio               | -       | 8.69      |

## 2.4. TiO<sub>2</sub> Physical Properties

**Table 2** provides a detailed overview of the physical properties of the TiO<sub>2</sub>/water nanofluid used in the experimental investigation, emphasizing key characteristics that influence its effectiveness as a heat transfer fluid. The average particle size of the TiO<sub>2</sub> nanoparticles was measured to be less than 100 nm, a crucial factor for enhancing thermal conductivity and ensuring stability within the base fluid. The high purity of the nanoparticles, exceeding 99%, minimized impurities that could otherwise affect the nanofluid's performance. The specific heat capacity of the TiO<sub>2</sub>/water nanofluid was determined to be 3328 J/kg·K, which is a fundamental parameter influencing the amount of heat required to raise the fluid's temperature. This value, when compared to that of pure water, provides insight into the nanofluid's capability to store and transport thermal energy efficiently. The nanofluid's density was recorded at 1229 kg/m<sup>3</sup>, an important property for determining mass flow rates and fluid dynamics within the system. Additionally, the nanofluid exhibited a white coloration, a visual indicator of its dispersion and homogeneity within the water base. These properties collectively offer a comprehensive understanding of the TiO<sub>2</sub>/water nanofluid's physical attributes, providing critical data for assessing its potential as an enhanced heat transfer medium in the parabolic trough collector system.

The thermophysical properties of the nanofluid were determined using validated equations from previous research [21]. The density and specific heat capacity were calculated based on the following relationships in equations (1) and (2):



$$\rho_{nf} = \varphi \cdot \rho_{np} + (1 - \varphi) \cdot \rho_{bf} \quad (1)$$

$$c_{p,nf} = \frac{\rho_{bf} \cdot (1 - \varphi)}{\rho_{nf}} \cdot c_{p,bf} + \frac{\rho_{np} \cdot \varphi}{\rho_{nf}} \cdot c_{p,np} \quad (2)$$

where  $\rho_{nf}$  is the nanofluid density (kg/m<sup>3</sup>),  $\rho_{np}$  is the nanoparticle density (kg/m<sup>3</sup>),  $\rho_{bf}$  is the base fluid density (kg/m<sup>3</sup>),  $c_{p,nf}$  is the nanofluid specific heat capacity (J/kg·K),  $c_{p,np}$  is the base fluid-specific heat capacity (J/kg·K),  $c_{p,bf}$  is the nanoparticle specific heat capacity (J/kg·K), and  $\varphi$  is the volume fraction of the nanofluid.

**Table 2.** Physical properties of the TiO<sub>2</sub>/Water nanofluid used in the experiment.

| Property                | Unit              | TiO <sub>2</sub> /Water Nanofluid |
|-------------------------|-------------------|-----------------------------------|
| Particle size (Average) | nm                | <100                              |
| Purity                  | %                 | >99                               |
| Specific Heat Capacity  | J/kg·K            | 3328                              |
| Density                 | kg/m <sup>3</sup> | 1229                              |
| Color                   | –                 | White                             |

The experimental setup included a continuous closed-loop system with a pump circulating the heat transfer fluids through the absorber tube. A manual valve at the outlet regulated the flow rate. Solar radiation tracking was performed manually throughout the experiment, which was conducted between 11:00 AM and 2:00 PM over three consecutive days in Guemar, El-Oued, Algeria.

The thermal efficiency of the collectors was analyzed based on temperature measurements recorded at 20-minute intervals for each heat transfer fluid. The ambient temperature and wind speed were also considered, as these factors influence heat loss and collector efficiency. Solar irradiation data was obtained from the SOLCAST website.

To evaluate the thermal efficiency, the useful heat absorbed by the working fluids was calculated using the heat transfer equation [22] (equation (3)):

$$Q_u = \dot{m}Cp(T_{out} - T_{int}) \quad (3)$$

where  $Q_u$  is the absorbed heat flux,  $\dot{m}$  is the mass flow rate,  $Cp$  is the specific heat capacity of the heat transfer fluid, and  $T_{out}$  and  $T_{in}$  are the outlet and inlet temperatures, respectively.

The efficiency of the PTCs was then determined using the following equation (4) [22]:

$$\eta_{exp} = \frac{Q_u}{DNI \cdot A_a} \quad (4)$$

where  $\eta_{exp}$  is the thermal efficiency of the PTC,  $DNI$  is the Direct Normal Irradiance, and  $A_a$  is the aperture area of the collector.

This methodology allowed for a comparative evaluation of the thermal efficiency of water and TiO<sub>2</sub>-based nanofluid as heat transfer fluids under real environmental conditions.

### 3. RESULTS AND DISCUSSION

#### 3.1. Case 1: Flow Rate = 0.4 L/min

##### 3.1.1. Thermal efficiency

**Figure 3** presents a comparative analysis of the thermal efficiency of distilled water (DW) and a 0.3% TiO<sub>2</sub>-water nanofluid under varying direct normal irradiance (DNI) conditions at a flow rate of 0.4 L/min. The data reveal a direct correlation between DNI and thermal efficiency for both fluids, confirming that increased solar radiation significantly enhances heat

absorption. The TiO<sub>2</sub> nanofluid consistently outperformed DW, maintaining an approximate 9% higher thermal efficiency throughout the experiment. The maximum efficiency of the nanofluid reached 40%, compared to DW's peak efficiency of 31%.

This enhanced performance is attributed to the superior heat transfer properties of the nanofluid, facilitated by the presence of TiO<sub>2</sub> nanoparticles, which improve thermal conductivity and convective heat transfer. The highest DNI recorded during the experiment was 873 W/m<sup>2</sup>, occurring around midday, which corresponded to the peak thermal efficiency for both fluids. The nanofluid system effectively leveraged this increased solar input, sustaining higher efficiency levels during peak DNI hours.

As DNI decreased in the late afternoon, the thermal efficiencies of both fluids gradually converged. This convergence occurred because the reduced solar radiation limited heat absorption, diminishing the relative advantage of the nanofluid. These findings underscore the potential of TiO<sub>2</sub>-water nanofluid as an enhanced heat transfer medium for improving the performance of parabolic trough collectors, particularly in high solar irradiance environments.

**Figure 3** also effectively illustrates the dynamic relationship between solar irradiance and thermal performance, emphasizing the advantages of using nanofluids to enhance heat transfer in solar thermal systems. The sustained efficiency gain observed with the TiO<sub>2</sub>-water nanofluid, particularly during peak irradiance periods, underscores its potential to optimize the overall performance of parabolic trough collectors. Because the nanofluid exhibits superior thermal conductivity and enhanced convective heat transfer, it effectively captures and retains more thermal energy compared to distilled water. This advantage is especially pronounced during periods of high DNI, where the nanofluid maintains greater thermal efficiency. These findings suggest that integrating nanofluids into solar collector systems can lead to significant improvements in heat absorption and utilization, making them a promising alternative for enhancing solar thermal energy conversion in high-irradiance environments.

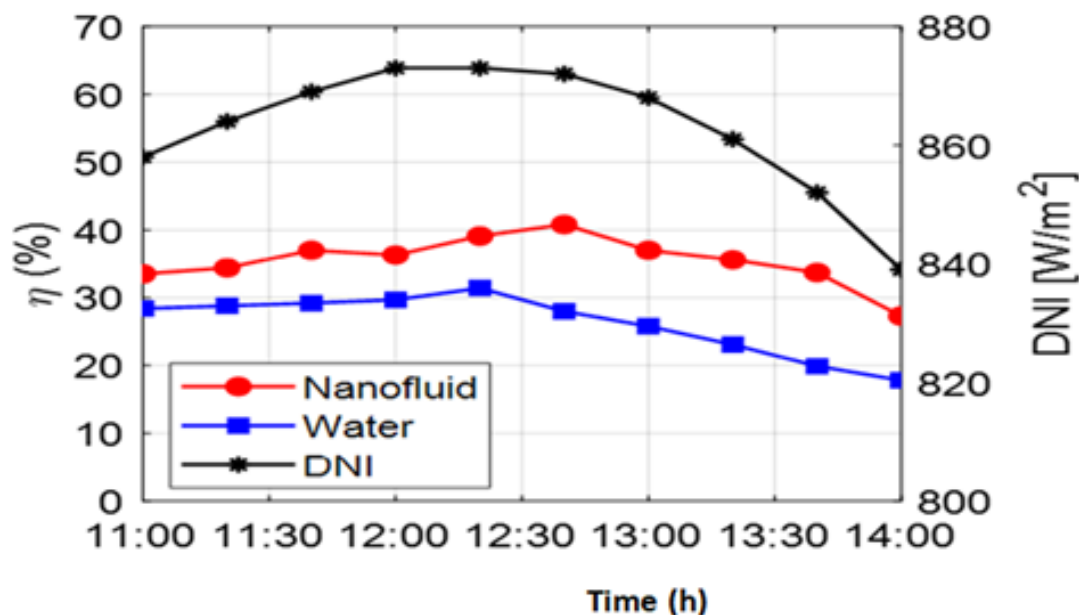


**Figure 3.** Thermal efficiency vs. average direct solar irradiance at 0.4 L/min flow rate.

### 3.1.2. Outlet temperature

**Figure 4** illustrates the temporal variation of outlet temperatures for the TiO<sub>2</sub> nanofluid and distilled water, demonstrating the enhanced heat absorption and retention properties of the nanofluid. The curves, recorded from 11:00 to 14:30, exhibit a consistent trend in which

the nanofluid maintains a higher outlet temperature than distilled water throughout the experiment. This persistent temperature difference confirms the superior thermal conductivity and improved heat transfer characteristics facilitated by the presence of  $\text{TiO}_2$  nanoparticles. Both fluids experience a rapid increase in outlet temperature during the initial hours, reaching peak values between 60 and 63°C from 12:00 to 12:30, a period that corresponds to the maximum solar radiation. This correlation between peak solar intensity and fluid temperature highlights the direct influence of solar irradiance on thermal performance. The nanofluid consistently maintains a slightly higher temperature during this peak period, further substantiating its improved heat absorption efficiency.

As solar intensity declines in the afternoon, the outlet temperatures of both fluids exhibit a gradual decrease. The similar downward trend observed in both curves reinforces the direct dependence of outlet temperature on solar radiation levels. However, the sustained temperature differential between the two fluids emphasizes the prolonged heat retention advantage of the  $\text{TiO}_2$  nanofluid. This consistent thermal enhancement suggests that integrating nanofluids into solar thermal applications can significantly improve system efficiency by maximizing heat absorption and retention, particularly in high-irradiance environments.

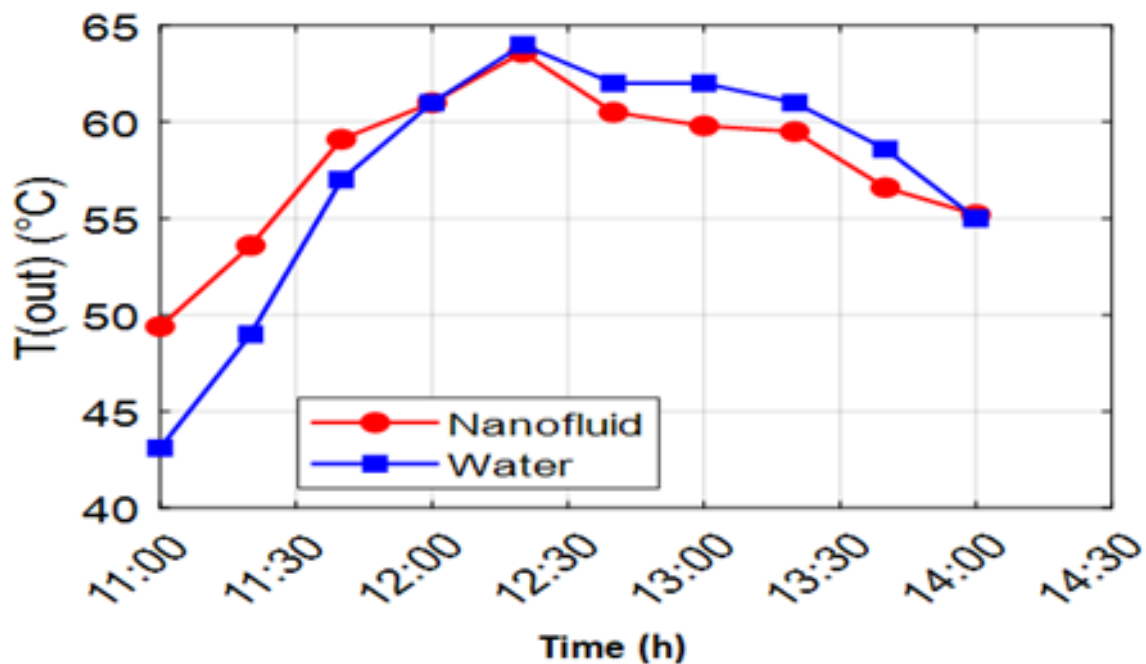


**Figure 4.** Outlet temperature comparison of distilled water and  $\text{TiO}_2$  nanofluid at 0.4 L/min flow rate.

### 3.1.3. Ambient temperature variations

**Figure 5** tracks ambient temperature fluctuations throughout the experimental study, providing crucial context for evaluating the performance of the PTCs. The data, recorded at a constant flow rate of 0.4 L/min, indicate a relatively stable ambient temperature profile, fluctuating between 30 and 37°C. This limited variation is highly desirable in experimental conditions because it minimizes the influence of external temperature fluctuations on the thermal performance of the PTCs. By maintaining a stable ambient temperature, the study effectively isolates the impact of the key variable under investigation: the working fluid. This controlled environment ensures that the observed differences in thermal efficiency between



distilled water and the  $\text{TiO}_2$  nanofluid are primarily attributable to the fluid's thermophysical properties rather than external temperature fluctuations. Consequently, the experiment provides a reliable assessment of the nanofluid's effectiveness in enhancing heat transfer performance in solar thermal applications.

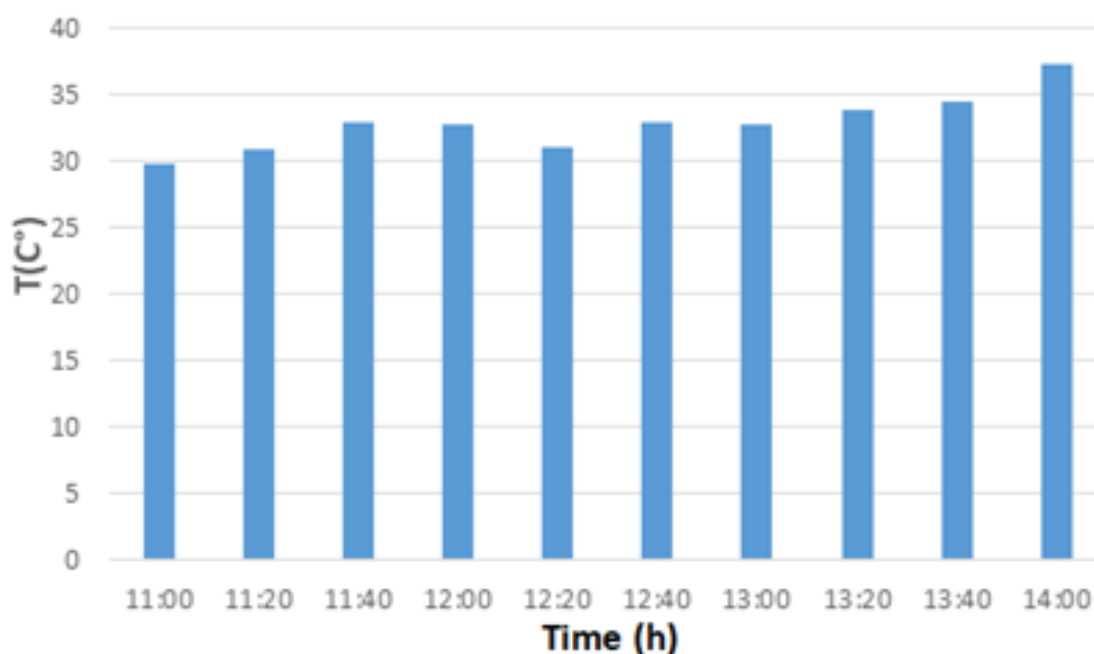


**Figure 5.** Ambient temperature variations during the experiment at 0.4 L/min flow rate.

### 3.1.4. Average wind speed

**Figure 6** illustrates the average wind speed recorded during the experimental period at a constant flow rate of 0.4 L/min, providing critical insights into the heat transfer dynamics of the PTCs. The data reveal a remarkably stable wind speed of 3 m/s for most of the experiment, from 11:00 to 13:40. This stability is significant because wind speed directly affects convective heat loss from the absorber tube. A constant wind speed ensures that the rate of convective heat loss remains steady, allowing for a more accurate assessment of the thermal performance of the working fluids. By maintaining a stable wind speed, the study effectively minimizes the influence of external convective cooling, ensuring that differences in thermal efficiency between distilled water and the  $\text{TiO}_2$  nanofluid are primarily due to variations in fluid properties. Towards the end of the experiment, at 14:00, a slight increase in wind speed to 3.1 m/s is observed. Although minor, this fluctuation highlights the dynamic nature of environmental conditions and their potential impact on heat transfer. However, given the small magnitude of this variation, its effect on overall heat loss is expected to be negligible. The data presented in **Figure 6** thus support the conclusion that the observed improvements in thermal performance result from the superior thermophysical properties of the nanofluid rather than external environmental factors.

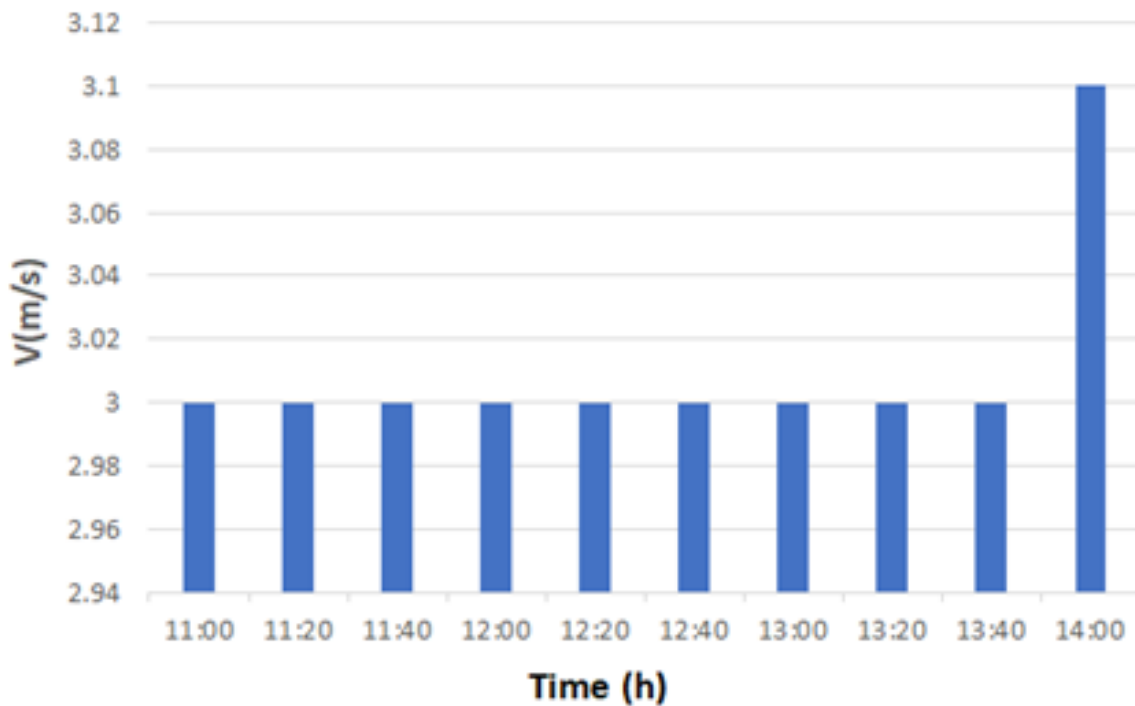


**Figure 6.** Average wind speed recorded during the experiment at 0.4 L/min flow rate.

### 3.2. Case 2: Flow Rate = 0.3 L/min

#### 3.2.1. Thermal efficiency

**Figure 7** presents a comparative analysis of the thermal efficiency of TiO<sub>2</sub>-water nanofluid and distilled water at a reduced flow rate of 0.3 L/min under varying direct normal irradiance (DNI) conditions. The curves illustrate a clear correlation between DNI and thermal efficiency for both fluids, with efficiency increasing as DNI rises. At this lower flow rate, the TiO<sub>2</sub>-water nanofluid achieves a maximum efficiency of 36%, whereas the distilled water system reaches a peak efficiency of 29%. Despite the overall reduction in efficiency compared to the 0.4 L/min flow rate, the nanofluid consistently outperforms water, demonstrating its enhanced heat transfer capability. This performance advantage is attributed to the superior thermal conductivity and heat retention properties of the TiO<sub>2</sub> nanoparticles, which improve convective heat transfer within the working fluid. The maximum DNI recorded during the experiment was 854 W/m<sup>2</sup>, corresponding to the period of peak efficiency for both fluids. As DNI decreases later in the day, the thermal efficiency of both fluids declines, with a noticeable convergence in their performance. This trend highlights the critical role of solar input in determining the heat absorption and transfer efficiency of the PTC, while also reinforcing the benefits of nanofluids in sustaining higher thermal efficiency under varying operational conditions.

#### 3.2.2. Outlet temperature

**Figure 8** presents a detailed comparison of the outlet temperatures achieved by the TiO<sub>2</sub> nanofluid and distilled water at a reduced flow rate of 0.3 L/min, providing further evidence of the nanofluid's enhanced heat absorption and transfer capabilities. The results captured data from 11:00 to 14:30 in Guemar, El Oued province, Algeria. The nanofluid consistently maintains a higher outlet temperature than water throughout the experimental period. The data reveal a rapid increase in outlet temperature for both fluids during the first hours, culminating in a peak range of 61°C for the nanofluid and 58°C for water around 13:00. This

peak corresponds to the period of maximum solar radiation, indicating a direct correlation between solar intensity and fluid temperature. The higher peak temperature of the nanofluid underlines its superior heat absorption and retention properties. As the solar intensity decreases in the afternoon, both fluids experience a gradual decrease in outlet temperature. This downward trend is consistent with the reduction in DNI, reinforcing the direct dependence of the outlet temperature on solar irradiance. However, the nanofluid consistently maintains a temperature advantage throughout the decline, highlighting its ability to maintain higher temperatures even with reduced solar input.

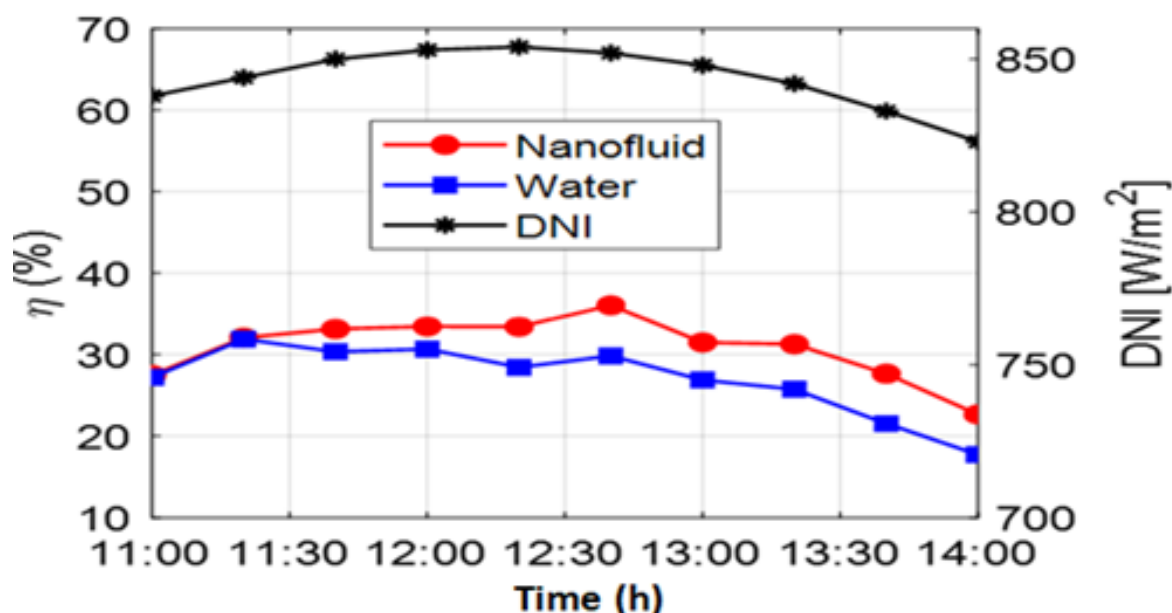


**Figure 7.** Thermal Efficiency vs. Direct Normal Irradiance (DNI) at 0.3 L/min Flow Rate.

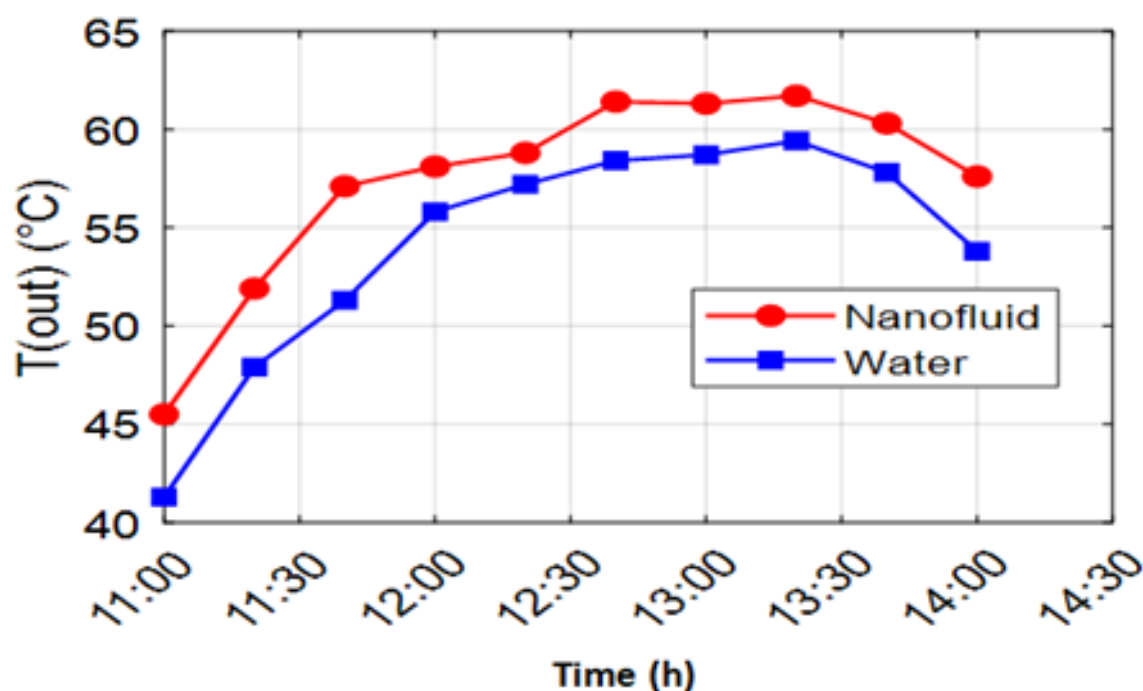


**Figure 8.** Outlet Temperature Comparison of Distilled Water and  $\text{TiO}_2$  Nanofluid at 0.3 L/min Flow Rate.

### 3.2.3. Ambient temperature variations

**Figure 9** illustrates the ambient temperature variations recorded during the experimental period at a reduced flow rate of 0.3 L/min in Guemar, El Oued province, Algeria. The data indicated a stable ambient temperature profile, fluctuating within a narrow range of 26 to 32°C. This stability is crucial for ensuring the reliability and accuracy of the experimental results, as it minimizes the influence of external temperature fluctuations on PTC performance. The consistency of ambient temperature reinforces the validity of the findings, confirming that improvements in thermal efficiency are primarily attributed to the TiO<sub>2</sub> nanofluid rather than external environmental factors. By mitigating the impact of temperature variations, the study establishes a robust foundation for assessing the effectiveness of nanofluids in enhancing solar thermal system performance. The data presented in **Figure 9** provide essential context for interpreting the thermal behavior of PTCs under varying operational conditions, supporting the conclusion that TiO<sub>2</sub> nanofluid significantly enhances heat transfer efficiency.

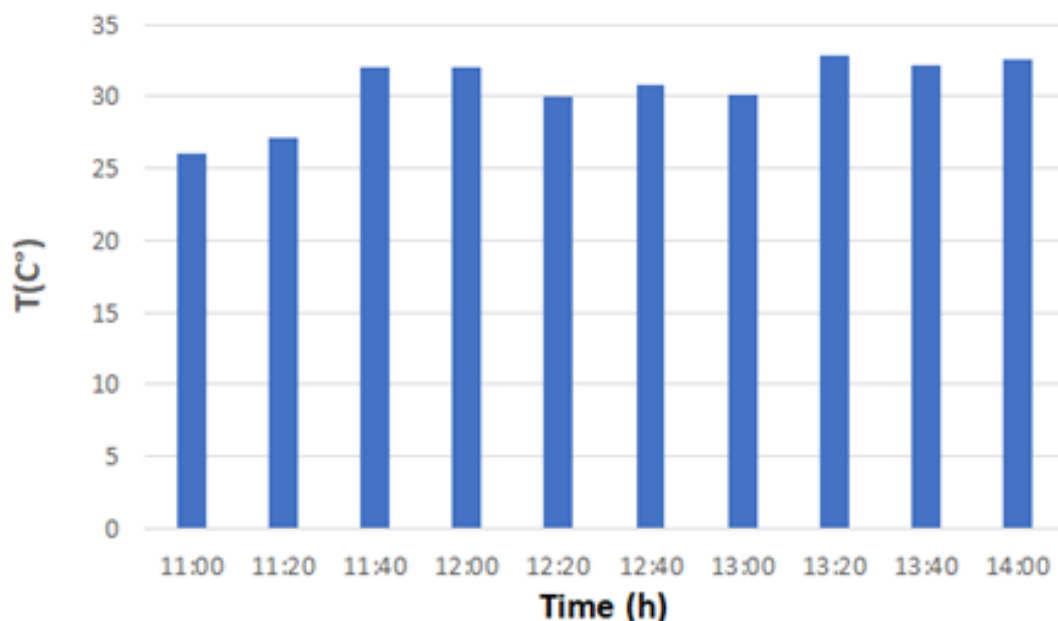


**Figure 9.** Ambient Temperature Variations During the Experiment at 0.3 L/min Flow Rate.

### 3.2.4. Average wind speed

**Figure 10** presents the average wind speed recorded throughout the experimental period at a reduced flow rate of 0.3 L/min, providing essential context for evaluating heat transfer dynamics in PTCs. The data revealed a stable wind speed of approximately 4.1 m/s from 11:00 to 13:00, which was significant because wind speed directly influenced convective heat loss from the absorber tube. This stability ensured that convective losses remained relatively constant, enabling a more accurate and controlled assessment of the thermal performance of the working fluids. After 13:00, a gradual decline in wind speed was observed, reaching 3.8 m/s by 14:00. While this reduction was noticeable, the overall variation remained within a narrow range, suggesting minimal impact on convective heat loss. The stability of wind conditions, particularly during peak solar irradiance, strengthened the validity of the experimental results. By minimizing external influences, the study provided a focused analysis of the TiO<sub>2</sub> nanofluid's intrinsic properties, demonstrating its role in enhancing heat retention and improving PTC thermal efficiency.

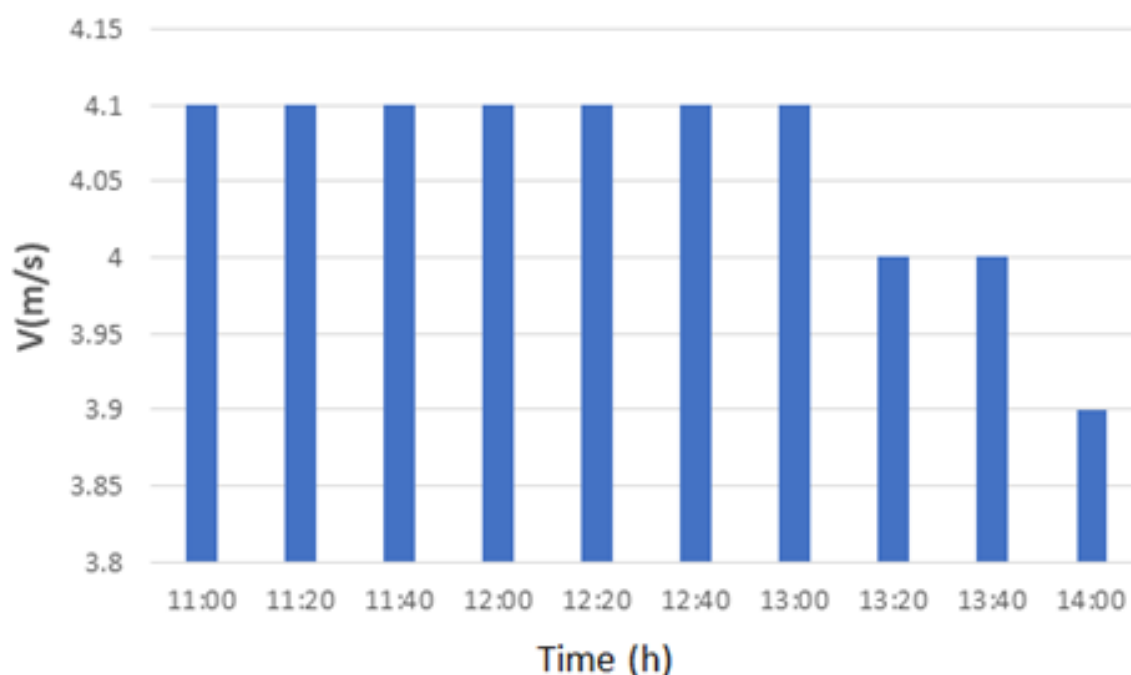


**Figure 10.** Average Wind Speed Recorded During the Experiment at 0.3 L/min Flow Rate.

### 3.3. Case 3: Flow Rate = 0.2 L/min

#### 3.3.1. Thermal efficiency

In this section, the experiments were conducted using a flow rate of 0.2 L/min. **Figure 11** presents a comparative analysis of the thermal efficiency between a  $\text{TiO}_2$  nanofluid and distilled water at this significantly reduced flow rate, under varying direct normal irradiance (DNI) conditions in Guemar, El Oued province, Algeria. The curves highlighted the profound impact of flow rate on the thermal performance of both fluids, revealing a notable decrease in overall efficiency compared to higher flow rate scenarios. At this minimum flow rate, the maximum efficiency achieved by the nanofluid system was 26%, while the water-based system reached a maximum of 21%. This reduction in efficiency was directly attributable to the lower recorded DNI, which peaked at approximately  $795 \text{ W/m}^2$ , indicating less available solar energy for heat absorption. Towards the final stages of the test, both fluids exhibited similar efficiencies. At extremely low flow rates, the thermal advantage of nanofluids over conventional fluids was significantly reduced. This observation highlighted the critical role of flow rate optimization in maximizing the benefits of nanofluids in solar thermal applications. While nanofluids demonstrated superior heat transfer properties, their effectiveness depended on maintaining adequate flow rates to minimize heat losses and fully utilize their enhanced thermophysical properties.

#### 3.3.2. Outlet temperature

**Figure 12** illustrates the temporal variation of the outlet temperatures of the  $\text{TiO}_2$  nanofluid and distilled water at a significantly reduced flow rate of 0.2 L/min, providing further evidence of the improved heat transfer performance of the nanofluid in Guemar, El Oued Province, Algeria. The curves demonstrated a consistent trend: the nanofluid exhibited a noticeably higher outlet temperature than water throughout the experimental period. The data revealed a gradual increase in the outlet temperature for both fluids during the first few hours, culminating in a peak of  $55^\circ\text{C}$  for the nanofluid and  $48^\circ\text{C}$  for water around 13:00. This peak corresponded to the period of maximum solar radiation, indicating a direct correlation



between solar intensity and fluid temperature. The nanofluid consistently maintained a slightly elevated temperature during this peak period, further validating its enhanced heat absorption capacity. As solar intensity decreased in the afternoon, both fluids experienced a gradual decline in outlet temperature. The decreasing trend was remarkably similar for both fluids. Although the nanofluid demonstrated higher heat absorption, both fluids responded similarly to changes in solar radiation. This synchronized decrease reinforced the direct dependence of outlet temperature on solar irradiance, while the consistent shift between the two curves highlighted the sustained thermal advantage of the  $\text{TiO}_2$  nanofluid. This data representation effectively illustrated the benefits of using nanofluids to improve heat transfer efficiency in solar thermal applications, even under challenging operating conditions.

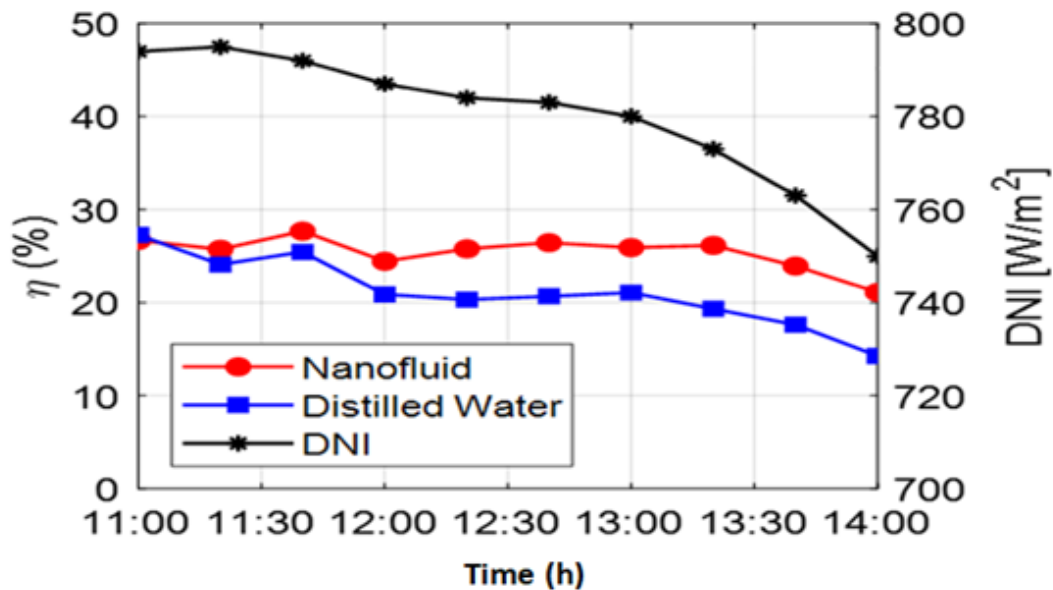


**Figure 11.** Thermal Efficiency vs. Direct Normal Irradiance (DNI) at 0.2 L/min Flow Rate.

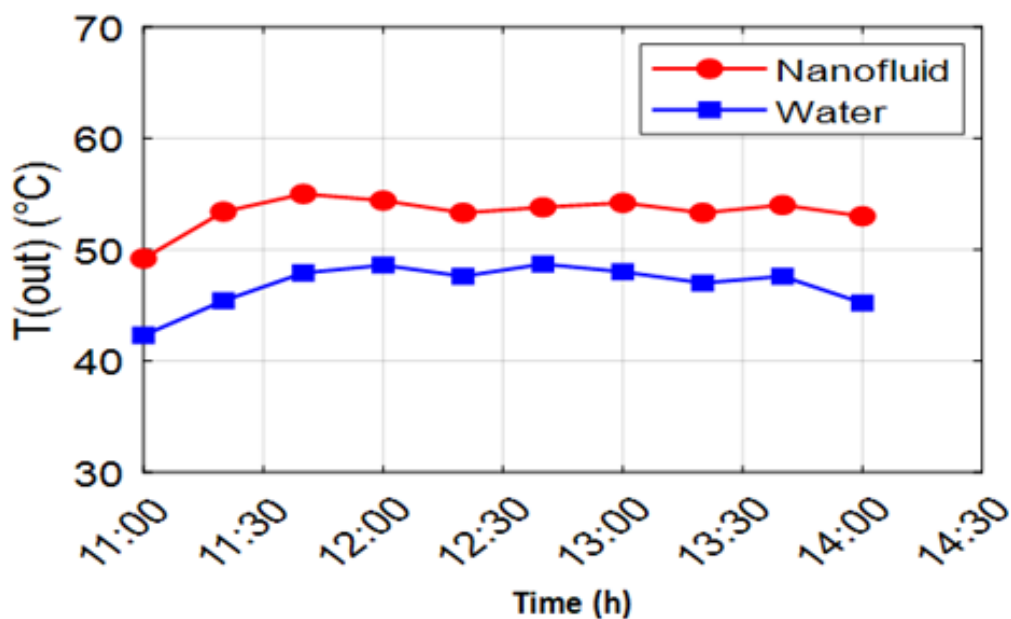


**Figure 12.** Outlet Temperature Comparison of Distilled Water and  $\text{TiO}_2$  Nanofluid at 0.2 L/min Flow Rate.

### 3.3.3. Ambient temperature variations

**Figure 13** documents the ambient temperature variations observed throughout the experimental period, conducted at a significantly reduced flow rate of 0.2 L/min in Guemar, El Oued Province, Algeria. The data revealed a remarkably stable ambient temperature profile, oscillating within a narrow range of 27 to 28°C for most of the experiment. This stability was crucial for ensuring the reliability and accuracy of the experimental results, as it minimized the influence of external temperature fluctuations on the performance of the PTCs. A slight peak of 29°C was observed at 14:00. While this increase was noticeable, the overall variation in ambient temperature remained within a very narrow range, and its impact on the thermal performance of the collectors was minimal. The stable ambient temperature profile reinforced the validity of the experimental findings, bolstering the claim that the TiO<sub>2</sub> nanofluid enhanced the thermal efficiency of PTCs. By minimizing external environmental interference, the study provided a robust foundation for concluding the efficacy of nanofluids in improving the performance of solar thermal systems. The data presented in **Figure 13** therefore served as a crucial component in the overall analysis, providing essential context for interpreting the observed thermal behavior of the PTCs under varying operating conditions, particularly at this low flow rate.

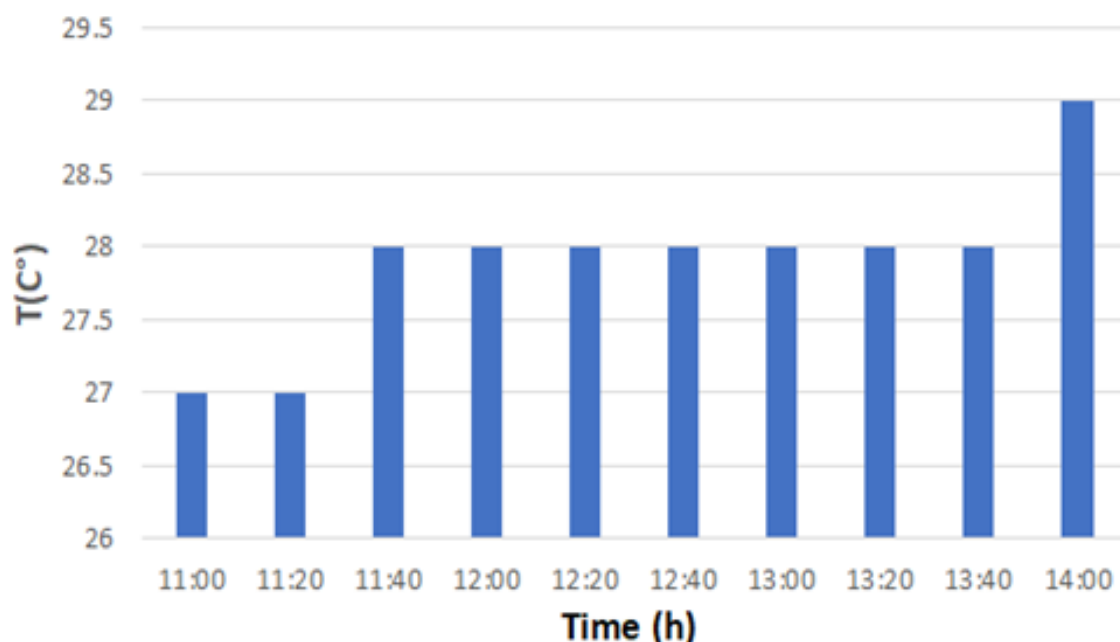


**Figure 13.** Ambient Temperature Variations During the Experiment at 0.2 L/min Flow Rate.

### 3.3.4. Average wind speed

**Figure 14** presents the average wind speed recorded during the experiment conducted at a significantly reduced flow rate of 0.2 L/min in Guemar, El Oued Province, Algeria. The data illustrated a distinct trend of decreasing wind speed throughout the experimental period, starting at approximately 6 m/s at 11:00 and gradually decreasing to 4 m/s at 14:00. This observation was crucial for understanding the heat transfer dynamics in PTCs. The high initial wind speed of 6 m/s indicated a substantial potential for convective heat loss from the absorber tube. Since wind speed directly influences the convective heat transfer rate, higher wind speeds generally lead to increased heat dissipation. The gradual decrease in wind speed therefore suggested a corresponding reduction in convective heat loss throughout the experiment. This declining wind speed likely played an important role in maintaining relatively

stable outlet temperatures in the  $\text{TiO}_2$  nanofluid-water system, even at low flow rates. The reduction in wind speed minimized heat dissipation, allowing the nanofluid to retain heat more efficiently than the water-based system, as observed in the outlet temperature data. The steady decrease in wind speed, while potentially beneficial for heat retention, also introduced a dynamic element into the experimental conditions. However, given the gradual nature of the decrease, its impact on the overall heat transfer dynamics was likely consistent throughout the period. The data presented in Figure 14 provided valuable support for the conclusion that the observed improvements in thermal performance were primarily attributable to the superior thermophysical properties of the nanofluid, rather than being significantly influenced by external environmental factors such as wind speed. Although the decrease in wind speed contributed to heat retention, it did not negate the observed performance advantage of the nanofluid.

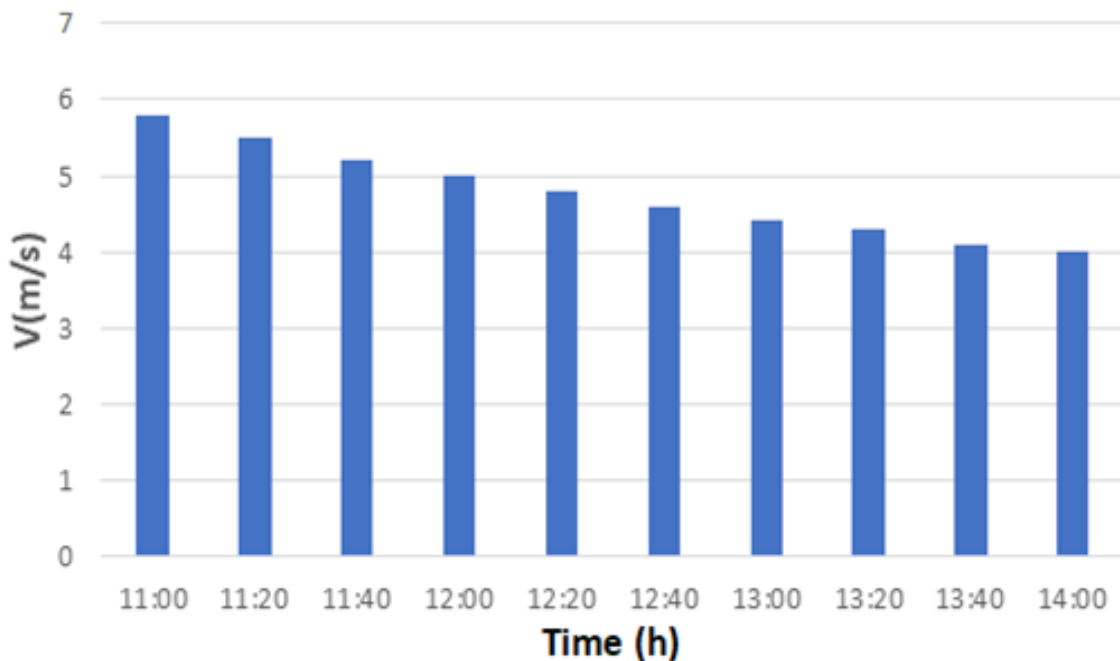


**Figure 14.** Average Wind Speed Recorded During the Experiment at 0.2 L/min Flow Rate.

### 3.4. Discussion

The study investigated the impact of  $\text{TiO}_2$  nanofluid on the thermal efficiency of PTCs across three distinct flow rates (0.4, 0.3, and 0.2 L/min). The results revealed a consistent trend: the nanofluid consistently outperformed distilled water, achieving higher peak efficiencies and maintaining higher outlet temperatures throughout the experimental period. This superior performance was attributed to the enhanced thermophysical properties of the nanofluid, particularly its higher thermal conductivity and improved heat retention capabilities. At the highest flow rate (0.4 L/min), the nanofluid achieved a peak efficiency of 40%, significantly exceeding the 31% recorded for distilled water. This substantial efficiency gain highlighted the potential of nanofluids to enhance solar thermal system performance. As the flow rate decreased, the efficiency advantage of the nanofluid persisted, though with diminished margins. At 0.3 L/min, the nanofluid achieved 36% efficiency compared to 29% for water, while at the lowest flow rate of 0.2 L/min, the nanofluid recorded 26% efficiency, exceeding the 21% achieved by water. This consistent pattern underscored the inherent advantages of nanofluids in PTCs. However, the decreasing efficiency gap between the

nanofluid and water at lower flow rates revealed a crucial insight: flow rate optimization is essential to fully maximize the performance benefits offered by nanofluids. Lower flow rates resulted in longer residence times within the absorber tube, leading to increased heat losses and a narrowing efficiency gap between the two working fluids. While this study demonstrated the superior thermal performance of TiO<sub>2</sub> nanofluid in PTCs, it also highlighted the necessity of carefully balancing flow rate considerations to fully exploit nanofluids' potential in solar thermal applications. The optimal flow rate depends on various factors, including PTC design, nanofluid concentration, and desired operating temperature. Future research should explore these parameters further to develop comprehensive guidelines for optimizing nanofluid-based solar thermal systems. This study adds new information regarding solar thermal energy, and the correlation is in good agreement with previous reports elsewhere [23-30].

#### 4. CONCLUSION

This study provides a comprehensive comparison of the thermal performance of PTCs using distilled water and TiO<sub>2</sub>-based nanofluid as heat transfer fluids under real environmental conditions in Guemar, El Oued, Algeria. The inclusion of TiO<sub>2</sub> nanoparticles significantly enhanced the heat transfer characteristics of the fluid, resulting in improved collector efficiency. Key findings from the experimental results are summarized as follows:

- (i) At the highest flow rate of 0.4 L/min, the TiO<sub>2</sub> nanofluid system achieved a peak thermal efficiency of 40%, compared to 31% for the water-based system, indicating a 9% improvement.
- (ii) With a flow rate of 0.3 L/min, the efficiency of the nanofluid system reached 36%, surpassing the water-based system, which achieved 29%, resulting in a 7% increase.
- (iii) At the lowest flow rate of 0.2 L/min, the nanofluid system achieved an efficiency of 26%, compared to 21% for the water-based system, reflecting a 5% gain in efficiency.
- (iv) Across all cases, the TiO<sub>2</sub> nanofluid exhibited higher outlet temperatures than water, with differences of up to 3 to 5°C during peak solar radiation.
- (v) The experimental data indicated that higher flow rates contributed to more effective heat transfer, with the efficiency gap between nanofluid and water narrowing as the flow rate decreased.

The findings confirm the critical role of solar radiation intensity and flow rate in determining thermal efficiency. The TiO<sub>2</sub> nanofluid consistently outperformed water across all experimental conditions, demonstrating superior heat absorption and retention capabilities. This study highlights the practical advantages of nanofluids in solar energy systems, particularly in arid regions with high solar exposure. These results contribute valuable insights into the development of advanced solar thermal systems. We obtained the efficiency improvements. TiO<sub>2</sub>-based nanofluids offer a viable solution for enhancing the performance of solar collectors, supporting sustainable energy generation in regions with extreme environmental conditions.

#### 5. ACKNOWLEDGMENTS

Belhadi Mohammed Abdelkrim, from Laboratoire des énergies Renouvelable et Développement Durable, Department of Mechanical Engineering, Faculty of Technology Sciences, University of Constantine 1, expresses his gratitude to the contributing researchers and the journal for publishing this article.

## 6. AUTHORS' NOTE

The authors declare that there is no conflict of interest regarding the publication of this article. The authors confirmed that the paper was free of plagiarism.

## 7. REFERENCES

- [1] Yilmaz, İ. H., and Mwesigye, A. (2018). Modeling, simulation and performance analysis of parabolic trough solar collectors: A comprehensive review. *Applied Energy*, 225, 135-174.
- [2] Bellos, E., and Tzivanidis, C. (2019). Alternative designs of parabolic trough solar collectors. *Progress in Energy and Combustion Science*, 71, 81-117.
- [3] Praveen, R. P., and Mouli, K. V. V. C. (2022). Performance enhancement of parabolic trough collector solar thermal power plants with thermal energy storage capability. *Ain Shams Engineering Journal*, 13(5), Article 101716.
- [4] Ma, X., Jin, R., Liang, S., Liu, S., and Zheng, H. (2020). Analysis of an optimal transmittance of Fresnel lens as a solar concentrator. *Solar Energy*, 207, 22-31.
- [5] Ghodbane, M., Benmenine, D., Khechekhouche, A., and Boumeddane, B. (2020). Brief on solar concentrators: Differences and applications. *Instrumentation Mesure Métrologie*, 19(5), 371-378.
- [6] Jebasingh, V. K., and Herbert, G. M. J. (2016). A review of solar parabolic trough collector. *Renewable and Sustainable Energy Reviews*, 54, 1085-1091.
- [7] Sun, J., Zhang, Z., Wang, L., Zhang, Z., and Wei, J. (2020). Comprehensive review of line-focus concentrating solar thermal technologies: Parabolic trough collector (PTC) vs linear Fresnel reflector (LFR). *Journal of Thermal Science*, 29(5), 1097-1124.
- [8] Dingding Y., Yujia Q., Yuanrui X., Kexin X., Yujie C., Xiaoping J., Kathleen B.A., Raymond R.T., Bohong W. (2024). Sequestration of carbon dioxide from the atmosphere in coastal ecosystems: Quantification, analysis, and planning. *Sustainable Production and Consumption*, 47, 413-424.
- [9] Bouhelal, M., Rouag, A., Bouhelal, A., and Belloufi, Y. (2023). Optimizing parabolic through collectors for solar stills: A 2D CFD parametric analysis. *International Journal of Energetica*, 8(2), 11-19.
- [10] Benhabib, L., Marif, Y., Hadjou Belaid, Z., Kaddour, A., Benyoucef, B., and Aillerie, M. (2021). Simulation of different modes of heat transfer on a parabolic trough solar collector. *International Journal of Energetica*, 6(2), 7-12.
- [11] Akilu, S., Sharma, K. V., Baheta, A. T., and Mamat, R. (2016). A review of thermophysical properties of water based composite nanofluids. *Renewable and Sustainable Energy Reviews*, 66, 654-678.
- [12] Hosseini, S. M. S., and Dehaj, M. S. (2021). An experimental study on energetic performance evaluation of a parabolic trough solar collector operating with Al<sub>2</sub>O<sub>3</sub>/water and GO/water nanofluids. *Energy*, 234, 121317.



- [13] Rehan, M. A., et al. (2018). Experimental performance analysis of low concentration ratio solar parabolic trough collectors with nanofluids in winter conditions. *Renewable Energy*, 118, 742-751.
- [14] Subramani, J., Sevvell, P., Anbuselvam, and Srinivasan, S. A. (2021). Influence of CNT coating on the efficiency of solar parabolic trough collector using AL<sub>2</sub>O<sub>3</sub> nanofluids - a multiple regression approach. *Materials Today: Proceedings*, 45, 1857-1861.
- [15] Bretado De Los Rios, M. S., Rivera-Solorio, C. I., and García-Cuellar, A. J. (2018). Thermal performance of a parabolic trough linear collector using Al<sub>2</sub>O<sub>3</sub>/H<sub>2</sub>O nanofluids. *Renewable Energy*, 122, 665-673.
- [16] Khalil, A., et al. (2020). Performance analysis of direct absorption-based parabolic trough solar collector using hybrid nanofluids. *Journal of the Brazilian Society of Mechanical Sciences and Engineering*, 42(11), 573.
- [17] Benrezkallah, A., Marif, Y., Soudani, M. E., Belhadj, M. M., Hamidatou, T., Mekhloufi, N., Aouachir, A. (2024). Thermal performance evaluation of the parabolic trough solar collector using nanofluids: A case study in the desert of Algeria. *Case Studies in Thermal Engineering*, 60, 104797.
- [18] Raza, S. H., et al. (2023). Experimental analysis of thermal performance of direct absorption parabolic trough collector integrating water based nanofluids for sustainable environment applications. *Case Studies in Thermal Engineering*, 49, 103366.
- [19] Ajay, K., and Kundan, L. (2016). Combined experimental and CFD investigation of the parabolic shaped solar collector utilizing nanofluid (CuO-H<sub>2</sub>O and SiO<sub>2</sub>-H<sub>2</sub>O) as a Working Fluid. *Journal of Engineering*, 2016, 1-11.
- [20] Sepahvand, P., Andalib, F. K., and Noori, S. (2022). Thermal efficiency enhancement of parabolic trough receivers using synthesized graphene oxide/SiO<sub>2</sub> nanofluid and a rotary turbulator. *International Journal of Sustainable Energy*, 41(7), 772-809.
- [21] Khanafer, K., and Vafai, K. (2011). A critical synthesis of thermophysical characteristics of nanofluids. *International Journal of Heat and Mass Transfer*, 54(19-20), 4410-4428.
- [22] Bellos, E., Tzivanidis, C., Antonopoulos, K. A., and Gkinis, G. (2016). Thermal enhancement of solar parabolic trough collectors by using nanofluids and converging-diverging absorber tube. *Renewable Energy*, 94, 213-222.
- [23] Laaraba, A., and Khechekhouche, A. (2018). Numerical simulation of natural convection in the air gap of a vertical flat plat thermal solar collector with partitions attached to its glazing. *Indonesian Journal of Science and Technology*, 3(2), 95-104.
- [24] Ahmad, F., Qurban, N., Fatima, Z., Ahmad, T., Zahid, I., Ali, A., Rajppot, S.R., and Maqbool, E. (2022). Electrical characterization of ii-vi thin films for solar cells application. *ASEAN Journal of Science and Engineering*, 2(2), 199-208.
- [25] Khamaia, D., Boudhiaf, R., Khechekhouche, A., and Driss, Z. (2022). Illizi city sand impact on the output of a conventional solar still. *ASEAN Journal of Science and Engineering*, 2(3), 267-272.

- [26] Bellila, A., Souyei, B., Kermerchou, I., Smakijk, N., Sadoun, A., Elsharif, N., and Siqueira A. (2024). Ethanol effect on the performance of a conventional solar still. *ASEAN Journal of Science and Engineering*, 4(1), 25-32.
- [27] Bhosale, S.K. (2022). Development of a solar-powered submersible pump system without the use of batteries in agriculture. *Indonesian Journal of Educational Research and Technology*, 2(1), 57-64.
- [28] Irawan, A.K., Rusdiana, D., Setiawan, W., Purnama, W., Fauzi, R.M., Fauzi, S.A., Alfani, A.H.F., and Arfiyogo, M.R. (2021). Design-construction of a solar cell energy water pump as a clean water source for people in Sirnajaya village, Gununghalu district. *ASEAN Journal of Science and Engineering Education*, 1(1), 15-20.
- [29] Kermerchou, I., Mahdjoubi, I., Kined, C., Khechekhouche, A., Bellila, A., and Isiordia, G.E.D. (2022). Palm fibers effect on the performance of a conventional solar still. *ASEAN Journal for Science and Engineering in Materials*, 1(1), 29-36.
- [30] Bellila, A., Khechekhouche, A., Kermerchou, I., Sadoun, A., Siqueira, A.M.D.O., Smakdji, N. (2022). Aluminum wastes effect on solar distillation. *ASEAN Journal for Science and Engineering in Materials*, 1(2), 49-54.